JOURNAL OF Materials CHEMISTRY

The effects of inherent solid particulates on the structure and mechanical properties of coal-tar pitch based C–C composites

E. Casal,[a] J. Viña,[b] J. Bonhomme,[c] M. Granda[a] and R. Menéndez*[a]

[a]*Instituto Nacional del Carbón, CSIC, Apartado 73, 33080 Oviedo, Spain*
[b]*Departamento Ciencia de los Materiales, Campus Universitario de Gijón, 33204 Gijón, Spain*
[c]*Instituto Tecnológico de Materiales de Asturias, 33428 Llanera (Asturias), Spain*

Received 22nd June 2000, Accepted 21st August 2000
First published as an Advance Article on the web 13th October 2000

Five unidirectional C–C composites were prepared using PAN-based carbon fibres and five pitches differing only in their inherent solid particles (QI) content. The results show that QI content affects the microstructure of the composite matrices The amount of smaller size crystalline structures (mosaic-like) increases with the increase of pitch QI content. On the other hand, QI particles also produce a significant increase in carbon yield, and consequently, composites show a higher percentage of carbon matrix. Mechanical properties, especially compressive strength, are also affected by the presence of QI particles. With the increase in QI content the mechanical properties of the composites are improved. However, this improvement always brings about a more brittle behaviour in the material, which is mainly due to the increase in the strength of fibre–matrix bonding. A good correlation between compressive and apparent interlaminar shear strength was found.

1. Introduction

Carbon fibre reinforced carbon–carbon composites (C–C composites) are recognized as advanced materials that have demonstrated great versatility in a wide variety of extreme performance situations due to their good thermo-mechanical properties at high temperature.[1,2] Coal-tar pitches are valuable products as carbon matrix precursors of C–C composites because of their low price, high carbon yield and excellent ease of conversion to graphite.[3] Industrially, coal-tar pitches are obtained by the fractionated distillation of tar, which is a by-product of metallurgical coke production.

The transformation of pitch into a carbon material requires a carbonization process. Coal-tar pitches are complex mixtures of organic compounds, with a highly aromatic character.[4] When heated, pitch softens and becomes liquid. Further heat treatment involves the release of volatiles and reactions of dehydrogenative polymerization and condensation, leading to large planar aromatic molecules (mesogens). The mesogens can be segregated from the isotropic pitch to give rise to a second liquid crystal phase known as a mesophase. As the mesophase becomes the continuous phase, the viscosity of the system increases rapidly and eventually the material solidifies into a coke (carbon which can be graphitized).[5] The optical texture of cokes (size, morphology and orientation of the crystalline structures observed under the microscope) and porosity contribute to the properties of the carbon material. The composition of the parent pitch and pyrolysis conditions affect the evolution of mesophase and therefore the optical texture of the coke.[6]

One of the industrial specifications of coal-tar pitches when they are for commercial use in the manufacture of electrodes is their quinoline insoluble content (QI). These QI are made up of carbonaceous particles, $<1\,\mu m$ in diameter, which are produced by the thermal cracking of volatile products during the coal coking process.[7] It is generally held that QI restrict the development and coalescence of the mesophase, so reducing the size of the crystalline structures and improving coke strength.[8,9] Provided that the presence of QI improves some of the properties of carbons *i.e.* strength, QI can be expected to have a beneficial influence on the structure and properties of C–C composites, when coal-tar pitch is used as a matrix precursor.

This paper reports on the influence of the QI content of a coal-tar pitch on the microstructural features and mechanical behaviour of unidirectional C–C composites. The use of a series of pitches prepared from the same coal-tar pitch but with different QI contents ensures that pitches will only differ in QI content.

2. Experimental

2.1. Material preparation

Two new pitches were prepared by blending a binder coal-tar pitch (11 wt% QI) with the same pitch, after reducing its QI to 0.5 wt% by filtration. Pitches are labelled according to their QI content: CTP-11 (parent pitch), CTP-7, CTP-3 and CTP-0 (filtered pitch). A fifth pitch, CTP-R, enriched in QI (54 wt%) was obtained from the residue of the filtration.

Pitch filtration was carried out as follows: 1000 g of CTP-11, placed in a stainless steel reactor, was heated to 250 °C and then passed through a 5 μm wire cloth twilled dutch weave filter pad (160 mm of diameter), using a pressure of 0.6 MPa of nitrogen.

The carbon fibre used (AS4-12k, Hercules Aerospace) was a commercial continuous, high-strength, high strain, PAN-based type, with a filament diameter of 7 μm. This fibre was surface-treated and sized.

2.2. Characterization of pitches

2.2.1. Elemental analysis. Carbon, hydrogen, nitrogen and sulfur contents were determined using a LECO CHNS 932 elemental analyzer. Oxygen contents were determined directly using a LECO.VTF-900 graphite furnace.

2.2.2. Quinoline solubility. The QI content was determined according to the ASTM D2318 standard. Two grams of pitch, <0.4 mm particle size, were placed in a 100 mL flask with

DOI: 10.1039/b005000h

25 mL of quinoline, and heated in a water bath to 75 °C for 20 minutes. The solution was filtered with a No 5 porous ceramic plate, and the residue washed with toluene and acetone for total quinoline removal.

2.2.3. Softening point. The softening point of the pitches was determined in a Mettler Toledo FP83HT Dropping Point Cell according to the ASTM D3104-87 standard. A small ring, 9 mm diameter, was filled with approximately 0.5 g of pitch. The ring was placed in the Mettler furnace and then pre-heated to 20 °C below the expected softening point. The oven temperature was then increased at a rate of 2 °C min^{-1} until the pitch flowed out of the ring, this representing the softening point of the pitch.

2.2.4. Carbon yield. Four grams of pitch, <0.4 mm particle size, was placed in a ceramic pot (42 mm id and 11 mm height) and carbonized in a horizontal furnace up to 900 °C at a rate of 5 °C min^{-1}, for 30 min, under a nitrogen flow of 56 mL min^{-1}. The carbon yield was calculated from the weight of the carbonaceous residue (coke).

2.3. Monitoring of pitch pyrolysis by hot-stage microscopy

About 200 mg of pitch was placed in a platinum crucible (7 mm id and 4 mm height) which was positioned in the heating stage of the microscope and heated at 10 °C min^{-1} under a nitrogen flow of 300 mL min^{-1}. Mesophase formation and development within the different pitches was monitored using a camera with an automatic exposure control.

2.4. Optical microscopy of cokes

Cokes obtained at 900 °C (section 2.2.4) were mounted in epoxy resin, successively ground on two grades of silicon carbide paper (600 and 1200 grits) and then polished with two different grades of alumina (0.3 and 0.05 μm) in an automatic grinding/polishing machine. Microscopic analysis was performed using a microscope with a 1λ retarder plate to produce interference colours to enable the identification of the shape, size and orientation of the crystalline structures which constitute their optical texture (mosaics <10 μm in diameter; domains <60 μm in length and <5 μm in width; and flow domains >60 μm in length and >10 μm in width[10]). Micrographs of representative areas of the samples were taken using oil-immersion objectives.

2.5. Composite preparation

Five plate-shaped unidirectionally reinforced composites were prepared by the wet-winding technique, using a procedure previously described,[11] which is similar to that of Rand.[12] CTP-0, CTP-3, CTP-7, CTP-11 and CTP-R coal tar pitches were used as matrix precursor for CC0, CC3, CC7, CC11 and CCR composites, respectively. Carbon fibres were impregnated with a solution/suspension of pitch in tetrahydrofuran (THF) and then wound on a rotating plate. An ultrasonic bath was used as pitch container to obtain a good homogenization and to prevent pitch segregation during the impregnation process. After removing the THF at 80 °C thin plates, 120 (fibre direction) × 65 × 1 mm were cut. Six of these plates were placed on top of each other in an open U-shaped mould. The heat treatment applied under an inert atmosphere was as follows: from room temperature at 5 °C min^{-1} to 480 °C for 1 hour and then at 1 °C min^{-1} to 650 °C. In the last stage a uniaxial pressure of 2 MPa was gradually applied and maintained for the rest of the process.

Additional carbonisation up to 1000 °C was performed in a horizontal tube furnace at 1 °C min^{-1} under a nitrogen flow of 65 mL min^{-1} (Fig. 1).

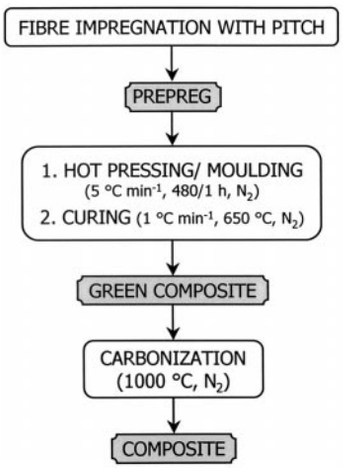

Fig. 1 Sequential steps followed in the preparation of unidirectional C–C composites.

2.6. Composite characterization

2.6.1. Optical microscopy and scanning electron microscopy. Samples of the composites were prepared for optical microscopy in the same way as the cokes (section 2.4). The analysis of each composite involved the percentage of fibres, matrix and pores, and the optical texture of the matrix.[10] The different structural features present in the composites were evaluated by a point-counting procedure on 500 points, statistically selected, using an oil-immersion objective of ×50 magnifications.

The fibre–matrix adhesion in the composites was studied using scanning electron microscopy (SEM), after etching with a chromic acid solution for 4 h.

2.6.2. Compressive and apparent interlaminar shear strength. Compression tests were carried out according to the ASTM D 3410 standard (Procedure B). The width of the samples was 10 mm and the speed of the test 1.2 mm min^{-1}. The compressive strength was quoted as the mean of the values from three specimens of each composite.

Interlaminar shear strength (ILSS) was calculated according to the ASTM D 2344-84 standard. Samples of 10 mm width were cut in the fibre direction and tested in a three point rig over a span of 12 mm between 3 mm diameter supporting rollers and a 6 mm diameter loading roller. The machine crosshead used was 1 mm min^{-1}. The results were quoted as the mean of five determinations.

3. Results and discussion

3.1. Influence of QI content on pitch properties

Table 1 shows the results of the characterization of the five pitches and the QI material. A similar elemental composition is

Table 1 Characteristics of pitches and QI material

	Elemental analysis (wt%)								
Sample	C	H	N	S	O	C : H[a]	CY/ wt%[b]	SP/ °C[c]	QI/ wt%[d]
CTP-0	93.0	4.3	1.0	0.6	1.3	1.8	44.6	119	0.5
CTP-3	93.5	4.3	1.0	0.6	1.3	1.8	46.2	118	3.3
CTP-7	93.7	4.1	1.0	0.6	1.2	1.9	48.2	119	7.3
CTP-11	93.6	4.0	1.0	0.6	1.2	2.0	47.8	114	11.0
CTP-R	93.6	3.1	0.9	0.7	1.8	2.5	69.8	—	47.0[e]
QI	93.8	2.2	0.7	0.7	2.4	3.6	94.7	—	—

[a]Carbon : hydrogen atomic ratio. [b]Carbon yield . [c]Softening point (Mettler). [d]Quinoline insolubles. [e]Estimated from the mass balance of the process.

observed for all the pitches, with the expected variations due to the different QI contents. This is further proof that the mild thermal conditions used in the filtration process have not significantly altered the chemical composition of the pitches, the minor differences being due to the QI material.

The QI material is characterised by a low H content, a high aromatic condensation degree as shown by its C : H atomic ratio, and a high carbon yield. Consequently, with increasing QI content, pitches exhibit lower H contents but higher C : H atomic ratios and carbon yields.

In the CTP-R the value of the softening point was not determined because the QI material hindered the flow of the pitch out of the ring. According to the standard procedure the QI content of this pitch was 54 wt%, which is higher than the 47 wt% calculated from the mass balance of the filtration. This discrepancy is due to the fact that the standard ASTM D2318 procedure is not suitable for such a high QI content, as some of the soluble fraction is retained by the QI.

3.2. Influence of QI on pitch pyrolysis behaviour

Variations in QI content have an important effect on the behaviour of pitches during pyrolysis, as can be observed by hot-stage microscopy. Despite the similar softening points, temperatures of mesophase initiation and hardening, the morphological characteristics of the mesophase developed by CTP-0 and CTP-11 are markedly different (Table 2).

In the initial stages of the pyrolysis (390 °C), small spheres of mesophase appear in CTP-0 which rapidly grow and coalesce. In CTP-11 the QI restrict the development of the mesophase because the QI particles surround the mesophase spheres, thereby preventing their growth and coalescence. This not only affects the amount of mesophase generated but also the shape and size of the spheres. The mesophase in CTP-0 is spherical with a wide range of sizes, while in CTP-11 the mesophase is very irregular in size and shape. This is because QI generate a viscous system in which the coalesced mesophase cannot recover its initial spherical shape. This phenomenon is more pronounced in CTP-R where a mesophase cannot be observed by hot-stage microscopy. Despite the different behaviour exhibited by CTP-0 and CTP-11, hardening takes place at the same temperature.

The optical texture of the cokes (Fig. 2a, 2b and 2c) is a clear consequence of the development of the mesophase explained above. Thus, the coke from CTP-0 shows an optical texture of flow domains. CTP-11 produces a coke with clusters of QI

Table 2 Hot-stage microscopy parameters for parent and filtered pitch

Pitch	SP/°C[a]	T_{mf}/°C[b]	T_H/°C[c]	ΔT/°C[d]	CR/wt%[e]
CTP-0	100	390	500	110	39.0
CTP-11	104	400	500	100	45.1

[a]Softening point. [b]Temperature of mesophase initiation. [c]Hardening temperature. [d]Difference between T_H and T_{mf}. [e]Carbonaceous residue at 600 °C.

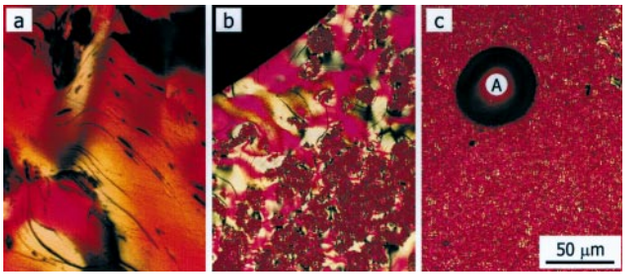

Fig. 2 Optical micrographs of cokes obtained from: (a) CTP-0, (b) CTP-11 and (c) CTP-R.

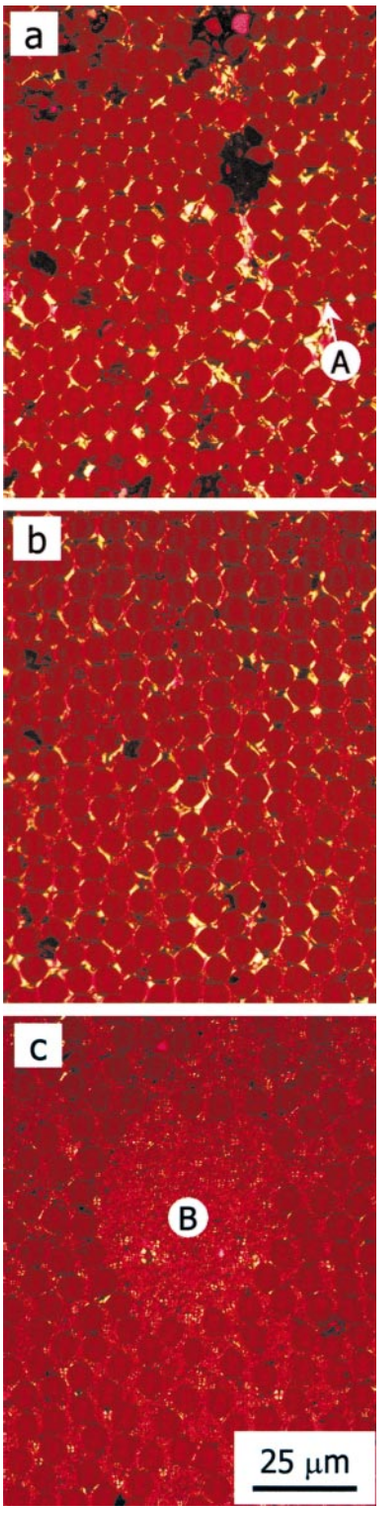

Fig. 3 Optical micrographs of cross-sections of composites: (a) CC0, (b) CC11 and (c) CCR.

particles embedded in the anisotropic phase, the main optical texture observed being that of domains. Finally, CTP-R generates a coke with an optical texture of fine mosaics, which is due to the high QI particle content.

Two main factors control the formation of voids in the coke: 1) gas evolution and 2) pitch viscosity during carbonization. CTP-R on carbonization loses fewer volatiles than CTP-0 and CTP-11, and generates a more viscous system. These two factors lead to a coke with a low porosity (34 vol% measured by optical microscopy) and rounded unconnected voids (Fig. 2c, position A). CTP-0 and CTP-11 originate cokes with a much

higher porosity (81.5 and 83.2 vol%, respectively) and a sponge-like structure of large interconnected voids.

3.3. Influence of the QI content on the preparation of C–C composites

The preparation of the composites was carried out according to the method described in the Experimental section (2.5). The pitch : THF ratio was in all cases 2 : 1. The suspension made out of pitch CTP-R was the most viscous. However this did not obstruct the preparation of the prepreg solution.

The weight of the prepreg solutions increased with the QI content of the precursor, ranging from 40 (CTP-0) to 60 g (CTP-R).

In the pressing/moulding step, the parameters were selected from the results of the hot-stage microscopic study which shows that the QI content causes an increase in the viscosity of the system. For this reason the temperatures chosen to begin application of mechanical pressure were the following: 505 °C for CC0; 500 °C for CC3; 495 °C for CC7; 490 °C for CC11 and 480 °C for CCR. In all cases there was some exudation of pitch. The transformation of the prepreg solutions into green composites produced a 50% reduction in thickness and simultaneously a 50% weight loss.

During carbonisation up to 1000 °C, composites underwent 1.5–2% of weight loss without any noticeable changes in their structure.

3.4. Influence of QI on the structure of C–C composites

Fig. 3 shows representative cross-sections of unidirectional composites obtained from the pitches. The optical texture of the matrix is in accordance with the features described in section 3.2. for the optical texture of the cokes. The structures vary from domains (Fig. 3a) in CC0 to very fine mosaics in CCR (Fig. 3c).

Fig. 4a shows that domains preferentially orientate themselves around the fibre. In the clusters of QI particles no order is observed (Fig. 4b). The clusters of QI disturb the spatial distribution of the fibres in the cross-section of the composite. This phenomenon is especially striking in CCR (Fig. 3c, position B) where the distribution of the fibre is very irregular.

The QI clusters cause a reduction in the contraction of the matrix during carbonisation. A similar effect was described for the addition of carbon particles (carbon black) to the precursors.[13,14] In CC0 the absence of QI leads to the formation of microcracks at the fibre–matrix interface (Fig. 3a, position A) probably due to the contraction of the large crystalline structures during carbonisation. When the QI content increases, the number of microcracks at the interface decreases. In CCR, no cracks at the interface were observed (Fig. 3c).

Percentages of fibre, matrix and porosity were determined by optical microscopy. The results are shown in Table 3. These values are the consequence of the combination of several parameters including the impregnation process, the carbon yield of the precursor, the variation in pitch viscosity during carbonisation and the temperature at which the mechanical pressure is applied. In CC0, the low carbon yield and the low viscosity of the pitch due to its low QI content, led to the highest percentage of fibre (77.3 vol%). On the other hand, CTP-R characterised by a high carbon yield and a high viscosity, produced a composite with a matrix content (48.4 vol%) even greater than that of the fibre (45.2 vol%).

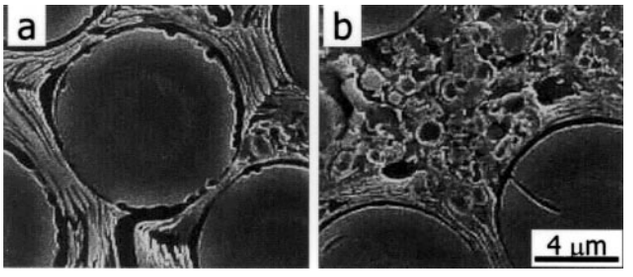

Fig. 4 SEM micrographs of the etched surfaces of composites: (a) CC0 and (b) CC11.

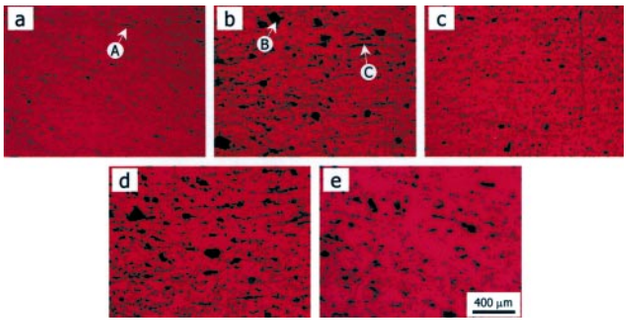

Fig. 5 Optical micrographs of cross-sections of composites: (a) CC0, (b) CC3, (c) CC7, (d) CC11 and (e) CCR.

Table 3 Microstructural features of composites

Composite	Fibre (vol%)	Matrix (vol%)	Porosity (vol%)
CC0	77.3	17.2	5.5
CC3	65.9	20.1	14.0
CC7	65.3	24.9	9.8
CC11	65.4	23.1	11.5
CCR	45.2	48.4	6.4

Fig. 5 gives an overall view of the porosity of the composites. In CC0 (Fig. 5a) voids of <50 µm in diameter are homogeneously distributed, which could be due to the high percentage of fibres (Table 3). These voids are preferentially oriented in a perpendicular direction to pressure application during composite moulding (Fig. 5a, position A). In CC3 voids of <50 µm in diameter coexist with larger voids of ~ 80 µm (Fig. 5b, position B). The tendency of the voids to be aligned is more pronounced in this composite than in CC0 (Fig. 5b, position C). CC7 is similar to CC0, although, as in CC3 voids of <50 µm and of ~ 80 µm are observed (Fig. 5c). CC11 resembles CC3 (Fig. 5d). Finally, CCR is characterized by a smaller amount of voids, these being mainly around 80 µm.

3.5. Influence of QI content on the mechanical properties of C–C composites

All the composites were mechanically tested in order to determine their interlaminar and compressive strength. The results are shown in Table 4.

Composites are materials which show a great dispersion of mechanical test results. This dispersion is even greater in the case of C–C composites due to their heterogeneity.[15] It is important therefore, to quote the standard deviation of the values obtained because this constitutes another property in itself. The number of specimens tested must be greater than 10. In this work, the limits imposed by production at laboratory scale restricted the number of specimens available for

Table 4 Mechanical properties of composites[a]

Composite	ILSS/MPa	Compressive strength/MPa
CC0	24.9 (3.8)	372.9 (37.8)
CC3	22.4 (3.2)	283.7 (43.6)
CC7	34.2 (6.4)	485.9 (63.9)
CC11	26.8 (0.9)	445.9 (63.9)
CCR	>35.9 (10.3)	515.0 (67.1)

[a]Numbers in parentheses refer to typical deviations.

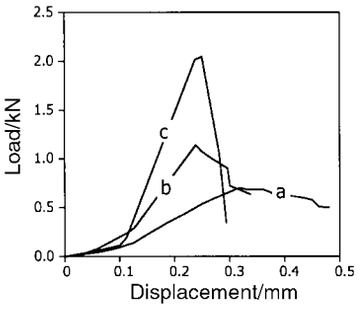

Fig. 6 Load–displacement curves of composites: (a) CC0, (b) CC11 and (c) CCR.

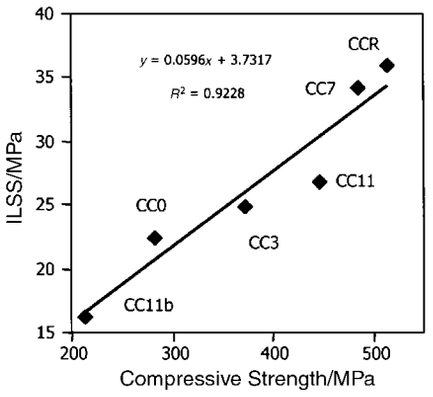

Fig. 7 Correlation of ILSS and compressive strength of composites: CC0, CC3, CC7, CC11 and CCR.

mechanical testing. The results shown in Table 4 are the mean of five samples (ILSS) and three samples (compression).

A. Apparent interlaminar shear strength. The fracture of CC0, CC3 and CC11 occurred in all cases by delamination, there being differences with respect to the mean value of 7–15%. CC7 failed under a mode that involved both flexion and shear mechanisms. CCR failed on flexion, a fact that influences the dispersion of the data obtained. The values calculated for this composite are not representative of the interlaminar shear strength which must be a lot higher.

Fig. 6 represents the load–displacement curves obtained from interlaminar shear testing. Although the QI content is not the only characteristic that varies from one composite to another, when comparing materials CC0, CC3, CC7, CC11 and CCR, it is clear that QI particles enhance the strength of the matrix–fibre bonding, resulting in an increase in shear strength but at the same time leading to a more brittle behaviour. This is in agreement with those authors who suggest that bonding at the interface is greater when the optical texture of the matrix is smaller (mosaics).[16,17]

A comparison of the values obtained from CC0 and CCR shows that this test depends on the characteristics of the matrix and the degree of fibre–matrix bonding. The percentage of fibre can be considered as a minor parameter, although it determines the physical area of the interface.

B. Compressive strength. It is generally held that tensile and flexural properties are fibre-dominated,[17] whereas density and matrix morphologies mainly affect compression behaviour. Therefore, compression seems to be an appropriate test for revealing the effects of QI content on the mechanical behaviour of the composites. CC7, again, shows the greatest dispersion (Table 4). The overall tendency is for an increase in compressive strength with QI content.

A number of modes have been proposed in order to explain compression behaviour, but there is no really satisfactory account of compressive failure.[18] The failure modes observed in these samples varied from pure delamination in the outer layer to more complex mechanisms. It seems that there is a relationship between the modes observed in the short beam test and the ones under compression loads. Fig. 7 shows the correlation between apparent interlaminar shear strength and compressive strength. In this figure CC11b is also included. CC11b is a composite prepared in the same way as CC11, but with mechanical pressure applied at 480 °C. It is clear that compressive strength increases linearly with shear strength for a wide range of composites with a different matrix optical texture (from domains to mosaics), fibre content (77–45 vol%) and porosity (5.5–14 vol%). In these cases it must be inferred that the shear strength (a property that depends on porosity[19]) of the composite governs the compressive response. Such behaviour could be due to the amount or type of porosity in the composites (>5.5 vol%). Thus, in these composites, porosity could prevent the classical catastrophic failure currently observed under compression in composites with a lower void content,[20] giving rise to a matrix shear failure at lower loads than what might otherwise be expected.

4. Conclusions

QI particles play a major role in the development of mesophase during pitch pyrolysis. The coalescence of the spheres of mesophase is prevented by QI, producing matrices with a smaller size of optical texture and stronger fibre–matrix bonding.

An increase in QI content leads to an increase in shear and compressive strength in composites, modifying the modes of failure from pseudoplastic to brittle due to the increase in the strength of fibre–matrix bonding.

This study has demonstrated that the apparent interlaminar shear strength of composites is related to compression strength. A linear relationship between shear and compressive strength was observed.

References

1 G. Savage, *Chem. Ind.*, 1992, **20**, 525.
2 E. Fitzer, *Carbon*, 1987, **25**, 163.
3 B. Rand, in *Essentials of Carbon–Carbon Composites*, ed. C. R. Thomas, Royal Society of Chemistry, Cambridge, UK, 1993, pp. 67–102.
4 M. Zander, *Fuel*, 1987, **66**, 1536.
5 H. Marsh and P. L. Walker, in *Chemistry and Physics of Carbon*, ed. P. L. Walker and P. A. Thrower, Marcel Dekker Inc., New York, 1979, vol. 15, pp. 229–286.
6 J. J. Fernández, A. Figueiras, J. B. Parra, M. Granda, J. Bermejo and R. Menéndez, *Carbon*, 1995, **33**, 1235.
7 R. J. Gray and K. C. Krupinski, *Light Met.*, 1995, 583.
8 E. A. Heintz, P. W. Pysz, H. Marsh and R. Menéndez, *Proceedings of Carbon '88*, eds. B. Mc-Enaney and T. J. Mays, IOP Publishing Ltd., Bristol, UK, 1998, 268.
9 D. R. Ball, *Carbon*, 1987, **16**, 205.
10 M. A. Forrest and H. Marsh, in *Coal and Coal Products: Analytical Characterization Techniques*, ed. E. L. Fuller Jr., American Chemical Society, Washington, DC, Symposium Series, 1982, 205, p. 1.
11 A. Figueiras, J. J. Fernández, M. Granda, J. Bermejo, E. Casal and R. Menéndez, *J. Microsc.*, 1995, **177**, 218.
12 C. Ahearn and B. Rand, *Carbon*, 1996, **34**, 239.
13 W. Hüettner, in *Carbon Fibers Filaments and Composites*, ed. J. L. Figueiredo, C. A. Bernardo, R. T. K. Baker and K. J. Hüttinger, *NATO ASI Ser., Ser. E Appl. Sci.*, vol. 177, Kluwer Academic Publishers, Dordrecht, 1990, pp. 275–300.
14 R. Menéndez, J. J. Fernández, J. Bermejo, V. Cebolla, I. Mochida and Y. Korai, *Carbon*, 1996, **34**, 895.
15 F. Dillon, K. M. Thomas and H. Marsh, *Carbon*, 1993, **31**, 1337.
16 A. Figueiras, M. Granda, E. Casal, J. Bermejo, J. Bonhomme and R. Menéndez, *Carbon*, 1998, **36**, 943.
17 H. Weisshaus, S. Kenig and A. Siegmann, *Carbon*, 1991, **29**, 1203.
18 D. Hull, *An Introduction to Composite Materials*, Cambridge University Press, Cambridge, UK, 1990.
19 M. R. Wisnom, *Composites, Part A*, 1996, **27**, 17.
20 K. Hana, H. Hamada and Y. Nakanishi, *Compos. Sci. Technol.*, 1997, **57**, 1139.